Short communication: Field data imply that the sorting (D96/D50 ratios) of gravel bars in coarse-grained streams influences the probability of sediment transport

Running title: transport probability of coarse-grained material

Fritz Schlunegger, Romain Delunel and Philippos Garefalakis
Institute of Geological Sciences, University of Bern, 3012 Bern, Switzerland
+41 31 631 8767, schlunegger@geo.unibe.ch

Abstract

Conceptual models suggest that the mobility of fluvial gravel bars is mainly controlled by sediment discharge. Here we present field observations from streams in the Swiss Alps and the Peruvian Andes to document that for a given water runoff, the probability of bedload transport also depends on the sorting of the bed material. We calculate shear stresses that are expected for a mean annual water discharge, and compare these estimates with grain-specific thresholds. We find a positive correlation between the predicted probability of transport and the sorting of the bed material, expressed by the D_{96}/D_{50} ratio. These results suggest that besides sediment discharge, the bedload sorting exerts a measurable control on the gravel bar mobility.

1 Introduction

The dynamics and the mobility of gravel bars in coarse-grained streams exert a strong control on the channel form, where a large gravel bar mobility is commonly found in braided rivers, while a low mobility is associated with more stable channels (Church, 2006). Flume experiments (Dietrich et al., 1989) and numerical models (Wickert et al., 2013) have shown that sediment flux is one of the most important parameters, which controls the dynamics of these bars (Dade and Friend, 1998; Church, 2006) and which leaves a measurable impact in fluvial stratigraphies (Allen et al., 2013). Accordingly, a large sediment flux would increase the mobility of gravel bars and promote streams to adapt a braided pattern. In contrast, a low sediment flux is predicted to result in an armoring of the channel floor (Carling, 1981; Aberle and Nikora, 2006) through selective entrainment of finer-grained sediments (Whiting et al., 1988; Dietrich et al., 1989), thereby resulting in a better sorting of the channel bed material and in a stabilization and confinement of the channel-bar arrangement (Church, 2006). If this hypothesis was correct, one would also expect that well-sorted gravel bars should be less frequently reworked than poorly sorted one (Whiting et al., 1988), and that braided streams host gravel bars with a higher mobility probability than confined rivers. Here, we test this hypothesis with a focus on gravelly streams in the Swiss Alps where flow is confined in artificial channels, and in the Peruvian Andes where streams are braided. We selected gravel bars close to water gauging stations, determined the grain size distribution of these bars and calculated the probability of sediment transport for a selected water runoff, which in our case corresponds to the mean annual water discharge for comparison purposes. We explored whether

these flows are strong enough to shift the clasts that build the sedimentary framework of these bars. We thus considered the mobilization of these clasts as a condition, and thus as a threshold, for a change in the sedimentary arrangement of the target gravels bars. The braided character of streams in Peru complicates the calculation of the sediment transport probability mainly because of the large variability in channel widths and the occurrence of multiple active channels within a reach. For these streams, we therefore focused on a segment where all water flows in one single channel with a constant width over a c. 100 m-long reach. The research sites therefore offered conditions that are similar, or close, to a laboratory flume experiment (e.g., Dietrich et al., 1989) where channel metrics (width and gradient) are nearly stable, and where sediment transport, conditioned by grain size specific thresholds, mainly depends on water runoff and the related flow strength.

2 Methods and datasets

2.1 Entrainment of bedload material, and probability of sediment transport

Sediment mobilization occurs when flow strength τ exceeds a grain size specific threshold τ_c (e.g., Paola et al., 1992):

$$\tau > \tau_c \quad (1).$$

Threshold shear stress τ_c for the dislocation of grains with size D_x can be obtained using Shields (1936) criteria ϕ for the entrainment of sediment particles:

$$\tau_c = \phi(\rho_s - \rho)gD_x \quad (2),$$

where g denotes the gravitational acceleration and ρ_s and ρ the sediment and water densities, respectively. Assignments of values to ϕ vary and diverge between flume experiments (e.g., Carling et al., 1992; Ferguson, 2012; Powell et al., 2016) and field observations (Mueller et al., 2005; Lamb et al., 2008). We employ the full range between 0.03 and 0.06 (Dade and Friend, 1998), which considers most of the complexities including hiding and protrusion effects that are associated with sediment transport of coarse-grained material (e.g., Buffington and Montgomery, 1997; Whitaker and Potts, 2007; Wickert et al., 2013; Powell et al., 2016). It also accounts for the slope dependency of ϕ for most of the cases particularly where energy gradients are flatter than c. 0.01 (Bunte et al., 2013), as is generally the case here with a few exceptions (Table 1). Among the various grain sizes, the 84th percentile D_{84} has been considered to best characterize the sedimentary framework of a gravel bar (Howard, 1980; Hey and Thorne, 1986; Grant et al., 1990). Accordingly, flows that dislocate the D_{84} grain size are strong enough to alter the gravel bar architecture (Grant et al., 1990). We thus selected this threshold to quantify the minimum flow strengths τ_c to entrain the bed material. The use of the D_{50} (e.g., Paola and Mohrig, 1996) would yield in a lower threshold and thus in a greater transport probability.

Bed shear stress τ is computed through (e.g., Tucker and Slingerland, 1997):

$$\tau = \rho g R S \quad (3).$$

Here, S denotes the energy gradient, and R is the hydraulic radius, which is approximated through water depth d where channel widths $W > 20 \times d$ (Tucker and Slingerland, 1997), which is the case here. The combination of expressions for: (i) the continuity of mass including flow velocity V, channel width W and water discharge Q:

$$Q = VWd \quad (4);$$

(ii) the relationship between flow velocity and channel bed roughness n (Manning, 1891):

$$V = \frac{1}{n} d^{2/3} S^{1/2} \quad (5);$$

and (iii) an equation for the Manning's roughness number n (Jarrett, 1984):

$$n = 0.32 S^{0.38} d^{-1/6} \quad (6);$$

yields a relationship where bed shear stress τ depends on gradient, water flux and channel width (Litty et al., 2017):

$$\tau = 0.54 \rho g \left(\frac{Q}{W} \right)^{0.55} S^{0.935} \quad (7).$$

This equation is similar to the expression by Hancock and Anderson (2002), Norton et al. (2016) and Wickert and Schildgen (2019) with minor differences regarding the exponent on the channel gradient S and on the ratio Q/W. These mainly base on the different ways of how bed roughness is considered. The results, however, are similar.

We propagated the uncertainties in the variables (Table 1) using Monte Carlo simulations. Simulations were repeated 10'000 times, and the results are reported as percentage where $\tau > \tau_c$ during these iterations. These values then represent probabilities of sediment transport for a given water discharge.

2.2 Datasets

We collected grain size data from streams where water discharge has been monitored during the past years. These are the Kander, Lütschine, Rhein, Sarine, Simme, Sitter and Thur Rivers in the Swiss Alps (Fig. 1a). The target gravel bars are situated close to a water gauging station. At these sites, digital photographs were taken along or across a gravel bar with a Canon EOS PR. Grain sizes were measured with the Wolman (1954) method using the free software package ImageJ 1.52n (https://imagej.nih.gov). Following Wolman (1954), we used intersecting points of a grid to randomly select the grains to measure. A digital grid of 20x20 cm was thus placed on each photograph with its origin placed at the lower left corner of the photo. The intermediate or b-axis of approximately 250 – 300 grains situated beneath an interception point was measured at each location (gravel bar). In cases where more than half of the grain is buried, the neighboring grain was measured instead. If the same grain lay beneath several interception points, then the grain was only measured once. Only grains larger than a few millimeters could be measured. We complemented these data sets with published information on the D_{50}, D_{84} and D_{96} grain size (Litty and Schlunegger, 2017; Litty et al., 2017) for further streams in

Switzerland and Peru (Figs. 1a and 1b; Table 1). These authors used the same approach upon collecting grain size data, which justifies the combination of the new with the published datasets.

For the Swiss streams, channel widths and gradients (Table 1) were measured on orthophotos and LiDAR DEMs with a 2-m resolution provided by Swisstopo. We complemented this information with published values for channel width estimates for 21 Peruvian streams and for additional 5 streams in Switzerland (Table 1, please see references there). We added a 20% uncertainty on the morphometric variables, which considers the natural variability in gradients and channel widths along the study reaches. We likewise assigned an uncertainty of 20% to the grain size dataset, which considers a possible bias that could be related to the grain size measuring techniques (e.g., sieving in the field versus grain size measurements using the Wolman method; Watkins, 2019). It also considers a mean estimate for the temporal variability in the grain size data, as a repeated measurement on selected gravel bars in Switzerland has shown (Hauser, 2018). We considered that the Shields variable ϕ is equally distributed between 0.03 and 0.06 during the 10'000 iterations.

The Federal Office for the Environment (FOEN) of Switzerland has measured the runoff values of Swiss streams over several decades. We employed the mean annual discharge values over 20 years for these streams and calculated one standard deviation thereof (see Table 1). For the Peruvian streams, water discharges reported by Litty et al. (2017 and Reber et al. (2017) were used.

3 Results

The grain sizes range from 8 mm to 70 mm for the D_{50}, 29 mm to 128 mm for the D_{84}, and 52 mm and 263 mm to the D_{96}. The smallest and largest D_{50} values were determined for the Maggia and Rhein Rivers in the Swiss Alps, respectively (Table 1). The grain sizes in the Swiss Rivers also reveal the largest spread where the ratio between the D_{96} and D_{50} grain size ranges between 2.2 (Sarine) and 17.7 (Maggia Losone I), while the corresponding ratios in the Peruvian streams are between 2.1 (PRC-ME9) and 5.8 (PRC-ME17). In the Swiss Alps, the critical shear stresses τ_c (median values) for entraining the D_{84} grain size ranges from c. 20 Pa (Emme River) to c. 90 Pa (Rhein and Simme Rivers). In the Peruvian Andes, the largest critical shear values are <80 Pa (PRC-ME39). The shear stress values related to the mean annual water discharge (Q_{med}) range from c. 15 Pa to 100 Pa in the Alps and from 20 Pa to >400 Pa in the Andes. Considering the strength of a mean annual flow and the D_{84} grain size as threshold, the probability of sediment transport occurrence in the Peruvian Andes and in the Swiss Alps comprises the full range between 0% and 100%.

Rivers that are not affected by recurrent high magnitude events (e.g., debris flows) and where the grain size distribution is not perturbed by lateral material supply are expected to display a self-similar grain size distribution (Whittaker et al., 2011; D'Arcy et al., 2017; Harries et al., 2018),

characterized by a linear relationship between the D_{84}/D_{50} and D_{96}/D_{50} ratios. In case of the Maggia River, the largest grains are oversized if the D_{50} and the grain size distribution of the other streams are considered as reference (Fig. 2). This could either reflect a response to the high magnitude floods in this stream (Brönnimann et al., 2018), or to the supply of coarse-grained material by a tributary stream where the confluence is <1 km upstream of the Maggia sites. If we exclude the Maggia dataset, then the probability of sediment transport occurrence scales positively and linearly with the D_{96}/D_{50} ratios (Fig. 3). The observed relationship appears stronger for the Swiss rivers (R^2 = 0.74, p-value = 2E-4) than for the Peruvian stream (R^2 = 0.33, p-value = 4E-3). These correlations suggest that gravel bars with a poorer sorting of the bedload, here expressed by a high D_{96}/D_{50} ratio, have a greater probability for the occurrence of sediment transport than those with better-sorted material. Figure 3 also shows that for a given material sorting, the mobilization probability is greater in the Peruvian than in the Swiss rivers.

4 Discussion and Conclusions

The sediment transport calculation is based on the inference that floods are strong enough to entrain the frame building grain size D_{84}. Therefore, the relationships between the mobilization probability and the D_{96}/D_{50} ratio could depend on the selected grain size percentile (e.g., the D_{84} versus the D_{50}), which sets the transport threshold. However, this variable linearly propagates into the equation (2) and thus into the probability of $\tau > \tau_c$. Therefore, although the resulting probabilities vary depending on the threshold grain size, the relationships between the D_{96}/D_{50} ratio and the mobilization probability will not change. For the case where different discharge estimates are considered, here expressed as the ratio Δ of a specific runoff to the mean annual discharge Q_{med}, then the corresponding probability of sediment transport will change by $\sim \sqrt{\Delta}$ (equation 7), but the dependency on the D_{96}/D_{50} ratio will remain. This suggests that the sorting of the bed material has a measurable impact on the mobility of gravel bars and thus on the frequency of sediment mobilization irrespective of the selection of a threshold grain size and the choice of a reference water discharge. We note that while the data is relatively scarce and scattered (i.e., the same transport probability for c. twofold difference in the D_{96}/D_{50} ratio), the relationships observed between the probability of transport occurrence and the degree of material sorting are significant with p-values <<0.01. We explain the scatter in the data by the natural stochastic nature of processes that are commonly encountered in the field.

For a given D_{96}/D_{50} ratio, the probability of material transport is greater in the Peruvian than in the Swiss rivers. We explain this by the differences in the geomorphic conditions and sediment supply processes between both mountain ranges, and by the anthropogenic corrections of the Swiss streams. In the Swiss Alps, the channel network, the processes on the hillslopes, and the pattern of erosion and sediment supply has mainly been conditioned, and thus controlled, by the glacial impact on the landscape and the large variability of exposed bedrock lithologies (Salcher et al., 2014; Stutenbecker et al., 2016). In contrast, the erosion and sediment supply in the western Peruvian

189 Andes is mainly driven by the combined effect of orographic rain (Montgomery et al., 2001; Viveen
190 et al., 2019) and earthquakes (McPhilips et al., 2014). Because the patterns, conditions and
191 mechanisms of sediment supply largely influence the grain size distribution of the supplied material
192 (Attal et al., 2015), and as consequence, the downstream propagation of these grain size signals
193 (Sklar et al., 2006), we do not expect identical relationships between grain size parameters and
194 probability of sediment transport in both mountain ranges. In addition, all streams in Switzerland
195 are confined in artificial channels with a limited possibility for lateral shifts of gravel bars. The
196 confinement of runoff in artificial channels could thus enhance the armoring effect (Aberle and
197 Nikora, 2006), with the consequence that the sediment transport probability for a given flow
198 strength is likely to decrease, also because armoring results in a successive coarsening of the
199 material and in larger thresholds. Accordingly, the low sediment transport probability in the Alps
200 might have an anthropogenic cause, but a confirmation warrants further research. In Peru, channels
201 are braided within a broad channel belt. Therefore, the probability of a change in the bar-channel
202 arrangement is expected to be higher than in the confined Swiss streams. Despite these differences,
203 we predict that the sorting of coarse-grained bed sediments has measurable impacts on the mobility
204 of the bedload material. We therefore suggest that besides grain size, channel gradient, sediment
205 flux and transport regime (Dade and Friend, 1998; Church, 2006), the sorting of the bed material
206 represents an additional, yet important variable that influences the mobility of the gravel bars and
207 thus the stability of channels.
208
209 Figure 1
210 A) Map showing the sites where grain size data has been measured in the Swiss Alps. The research
211 sites are close to water gauging stations; B) map showing locations for which grain size and water
212 discharge data is available in Peru (Litty et al., 2017).
213
214 Figure 2
215 Relationship between ratio of the D_{96}/D_{50} and D_{84}/D_{50}, implying that the D_{96} grain sizes of the
216 Maggia gravel bars are too large if the D_{50} is taken as reference and if the other gravel bars are
217 considered.
218
219 Figure 3
220 Relationships between the probability of sediment transport occurrence and the D_{96}/D_{50} ratio, which
221 we use as proxy for the sorting of the gravel bar, in the Swiss and Peruvian rivers.
222
223 Table 1
224 Channel morphometry (width and gradient), grain size and water discharge measured at the research
225 sites. The table also shows the results of the various calculations (critical shear stress τ_c, shear stress
226 τ of a flow with a mean annual runoff Q_{med}, and probability of sediment transport occurrence related

to this flow).

Acknowledges

The Federal Office for the Environment (FOEN) is kindly acknowledged for providing runoff data for the Swiss streams.

References

Aberle, J. and Nikora, V.: Statistical properties of armored gravel bed surfaces, Water Resour. Res, 42, W11414, 2006.

Allen, P.A., Armitage, J.J., Carter, A., Duller, R.A., Michael, N.A., Sinclair, H.D., Whitchurch, A.L., and Whittaker, A.C.: The Qs problem: Sediment balance of proximal foreland basin systems, Sedimentology, 60, 102-130, 2013.

Attal, M., Mudd, S.M., Hurst, M.D., Weinmann, B., Yoo, K., and Naylor, N.: Impact of change in erosion rate and landscape steepness on hillslopes and fluvial sediments grain size in the Feather River basin (Sierra Nevada, California), Earth Surf. Dyn., 3, 201-222, 2015.

Bunte, K., Abt, S.R., Swingle, K.W., Cenderelli, D.A., and Schneider, M.: Critical Shields values in coarse-bedded steep streams, Water Res. Res., 49, 7427-7447, 2013.

Brönninmann, S., et al.: 1968 – das Hochwasser, das die Schweiz veränderte. Ursachen, Folgen und Lehren für die Zunkunft, Geographica Bernensai, G94, 52 p., 2018

Buffington, J. M. and Montgomery, D. R.: A systematic analysis of eight decades of incipient motion studies, with special reference to gravel-bedded rivers, Water Resour. Res., 33, 1993-2029, 1997.

Church, M.: Bed material transport and the morphology of alluvial river channels, Ann. Rev. Earth Planet. Sci., 34, 325-354, 2006.

Carling, P. A.: Armored versus paved gravel beds – discussion, J. Hydraul. Div., 107, 1117–1118, 1981.

Carling, P. A., Kelsey, A., and Glaister, M. S.: Effect of bed rough- ness, particle shape and orientation on initial motion criteria, in: Dynamics of gravel-bed rivers, edited by: Billi, P., Hey, R. D., Throne, C. R., and Tacconi, P., 23–39, John Wiley and Sons, Ltd., Chichester, 1992.

D'Arcy, M., Whittaker, A.C., and Roda-Bolduda, D.C.: Measuring alluvial fan sensitivity to past climate changes using a self-similarity approach to grain-size fining, Death Valley, California, Sedimentology, 64, 388-424, 2017.

Dade, B. and Friend, P.F.: Grain-size, sediment-transport regime, and channel slope in alluvial rivers, J. Geol., 106, 661-676, 1988.

Dietrich, W.E., Kirchner, J.W., Hiroshi, I., and Iseya, F.: Sediment supply and the development of the coarse surface layer in gravel-bedded rivers, Nature, 340, 215-217, 1989.

Ferguson, R.: River channel slope, flow resistance, and gravel entrainment thresholds, Water Resources Research, 48, W05517, 2012.

Grant, G. E., Swanson, F. J., and Wolman, M. G.: Pattern and origin of stepped-bed morphology in high gradient streams, western Cascades, Oregon, GSA Bull., 102, 340–352, 1990.

Hancock, G.S., and Anderson, B.S.: Numerical modeling of fluvial strath-terrace formation in response to oscillating climate, GSA Bull., 9, 1131-1142, 2002.

Harries, R.M., Kirstein, L.A., Whittaker, A.C., Attal, M., Peralta, S., and Brooke, S.: Evidence for self-similar bedload transport on Andean alluvial fans, Iglesia, basin, South Central Argentina, J. Geophys. Res. - Earth Surface, 123, 2292-2315, 2018.

Hauser, R.: Abhängigkeit von Korngrössen und Flussformen in den Schweizer Alpen, Unpubl. Ms thesis, Univ. Bern, Bern, Switzerland, 64 p., 2018.

Hey, R. D. and Thorne, C. R.: Stable channels with mobile gravel beds, J. Hydrol. Eng., 112, 671–689, 1986.
Howard, A. D.: Threshold in river regimes, in: Thresholds in geomorphology, edited by: Coates, D.R, and Vitek, J.D., Allen and Unwin, Boston, MA, 227-258, 1980.
Jarrett, R. D.: Hydraulics of high-gradient streams, J. Hydraul. Eng., 110, 1519-1939, 1984.
Lamb, M. P., Dietrich, W. E., and Venditti, J. G.: Is the critical Shields stress for incipient sediment motion dependent on channel bed slope? J. Geophys. Res., 113, F02008, 2008.
Litty, C. and Schlunegger, F.: Controls on pebbles' size and shape in streams of the Swiss Alps, J. Geol., 125, 101-112, 2017.
Litty, C., Schlunegger, F., and Viveen, W.: Possible threshold controls on sediment grain properties of Peruvian coastal river basins, Earth Surf. Dyn., 5, 571-583, 2017.
Manning, R.: On the flow of water in open channels and pipes, Trans. Inst. Civil Eng. Ireland, 20, 161–207, 1891.
McPhilips, D., Bierman, P.R., and Rood, D.H.: 2014, Millennial-scale record of landslides in the Andes consistent with earthquake trigger, Nature Geosci., 7, 925-930, 2014.
Montgomery, D. R., Balco, G., and Willett, S. D.: Climate, tectonics, and the morphology of the Andes, Geology, 29, 579–582, 2001.
Mueller, E. R., Pitlick, J., and Nelson, J. M.: Variation in the reference Shields stress for bed load transport in gravel- bed streams and rivers, Water Res. Res., 41, W04006, 2005.
Norton, K.P., Schlunegger, F., and Litty, C.: On the potential for regolith control of fluvial terrace formation in semi-arid escarpments, Earth Surf. Dyn., 4, 147-157, 2016.
Paola, C., Heller, P.L., and Angevine, C.: The large-scale dyanmics of grain size variation in alluvial basins, 1: Theory, Basin Res., 4, 73-90, 1992.
Paola, C. and Mohring, D.: Palaeohydraulics revisted: palaeoslope estimation in coarse-grained braided rivers, Basin Res., 8, 243-254, 1996.
Powell, M. D., Ockleford, A., Rice, S. P., Hillier, J. K., Nguyen, T., Reid, I., Tate, N. J., and Ackerley, D.: Structural properties of mobile armors formed at different flow strengths in gravel-bed rivers, J. Gephys. Res. – Earth Surface, 121, 1494-1515, 2016.
Reber, R., Delunel, R., Schlunegger, F., Litty, C., Madella, A., Akcar, N., and Christl, M.: Environmental controls on 10Be-based catchment-averaged denudation rates along the western margin of the Peruvian Andes, Terra Nova, 29, 282-293, 2017.
Salcher, B.C., Kober, F., Kissling, E., and Willett, S.D.: Glacial impact on short-wavelength topography and long-lasting effects on the denudation of a deglaciated mountain range, Global Planet. Change, 115, 59-70, 2014.
Shields A.: Anwendung der Ahnlichkeitsmekanik und der Turbulenzforschung auf die Geschiebebewegung, Mitt. Preuss. Versuch. Wasserbau Schiffbau, 26 p., Berlin, 1936.
Sklar, L.S., Dietrich, W.E., Foufoula-Georgiou, E.F., Lashermes, B., and Bellugi, D.: 2006, Do gravel bed river size distributions record channel network structure?, Water Res. Res., 42, W06D18, 2006.
Stutenbecker, L., Costa, A., and Schlunegger, F.: Lithological control on the landscape form from the upper Rhône Basin, Central Swiss Alps, Earth Surf. Dyn., 4, 253-272, 2016.
Tucker, G., and Slingerland, R.: Drainage basin responses to climate change, Water Res. Res, 33, 2031-2047, 1997.
Viveen, W., Zellavos-Valdivia, L., and Sanjurjo-Sanchez, J.: The influence of centennial-scale variations in the South American summer monsoon and base-level fall on Holocene fluvial systems in the Peruvian Andes, Gobal Planet. Change, 176, 1.22, 2019.
Watkins, S.: Linking source and sink in an active rift: quantifying controls on sediment export and depositional stratigraphy in the Gulf of Corinth, Central Greece, PhD thesis, Imperial College London, London, UK, 213 p., 2019.
Whitaker, A., and Potts, D.F.: Analysis of flow competence in alluvial gravel bed stream, Dupuyer

Creek, Montana, Water Res. Res., 43, W07433.
Whiting, P. J., Dietrich, W. E., Leopold, L. B., Drake, T. G., and Shreve, R. L.: Bedload sheets in heterogeneous sediment, Geology, 16, 105-108, 1988.
Whittaker, A.C., Duller, R.A., Springett, J., Smithells, R.A., Whitchurch, A.L., and Allen, P.A.: Decoding downstream trends in straigraphic grain size as a function of tectonic subsidence and sediment supply, GSA Bull., 123, 1363-1382, 2011.
Wickert , A.D., Martin, J.M., Tal, M., Kim, W., Sheets, B., and Paola, C.: River channel lateral mobility: metrics, time scales, and controls, J. Geophys. Res. - Earth Surface, 118, 396-412, 2013.
Wickert, A.D., and Schildgen, T.F.: Long-profile evolution of transport-limited gravel-bed rivers, Earth Surf. Dyn, 7, 17-43, 2019.
Wolman, M. G.: A method of sampling coarse riverbed material, Eos Trans AGU, 35, 951-956, 1954.

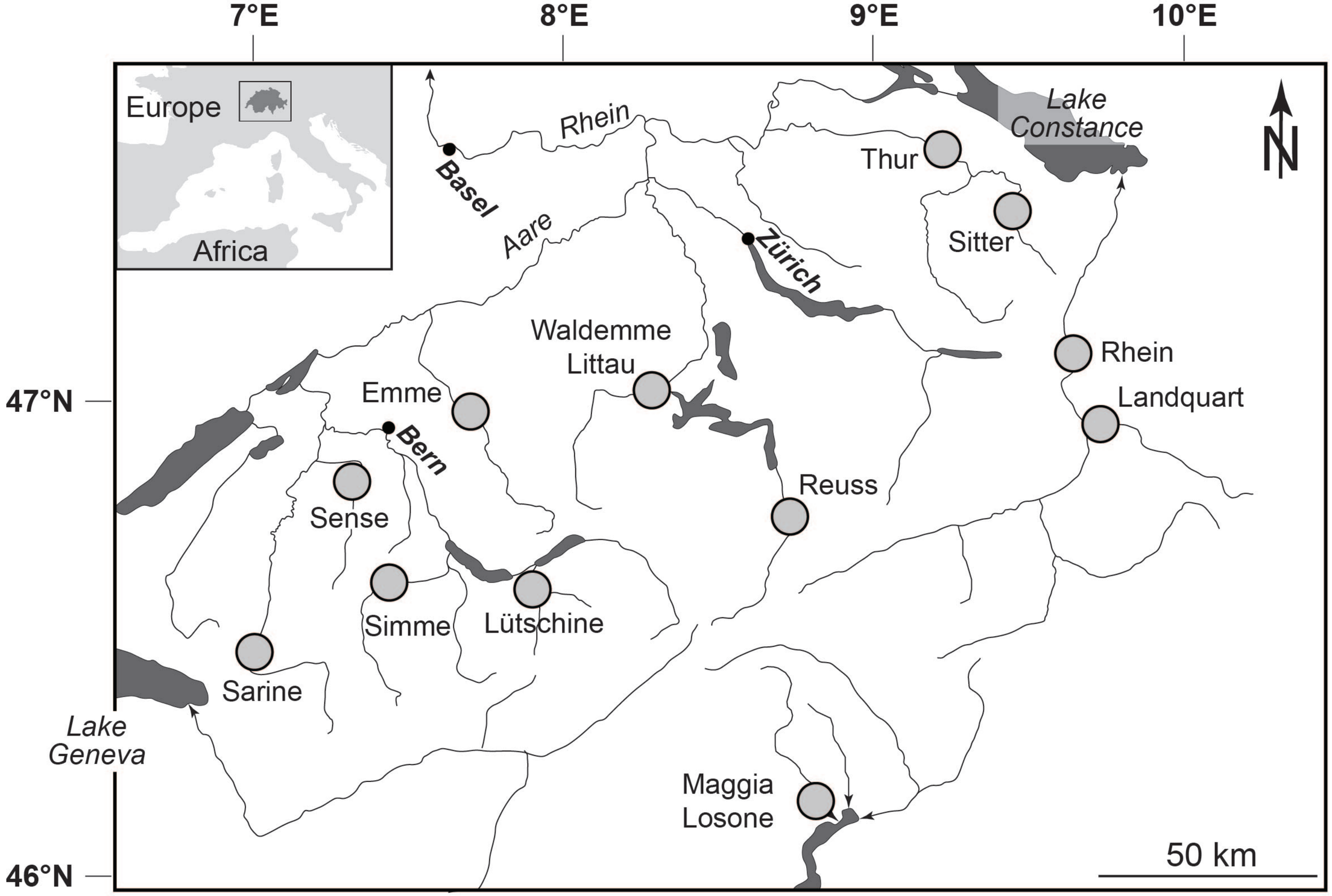
7°E
8°E
9°E
10°E
47°N
46°N
Europe
Africa
Rhein
Basel
Aare
Zürich
Lake
Constance
Thur
Sitter
Waldemme
Littau
Rhein
Landquart
Emme
Bern
Sense
Reuss
Simme
Lütschine
Sarine
Lake
Geneva
Maggia
Losone
50 km
A

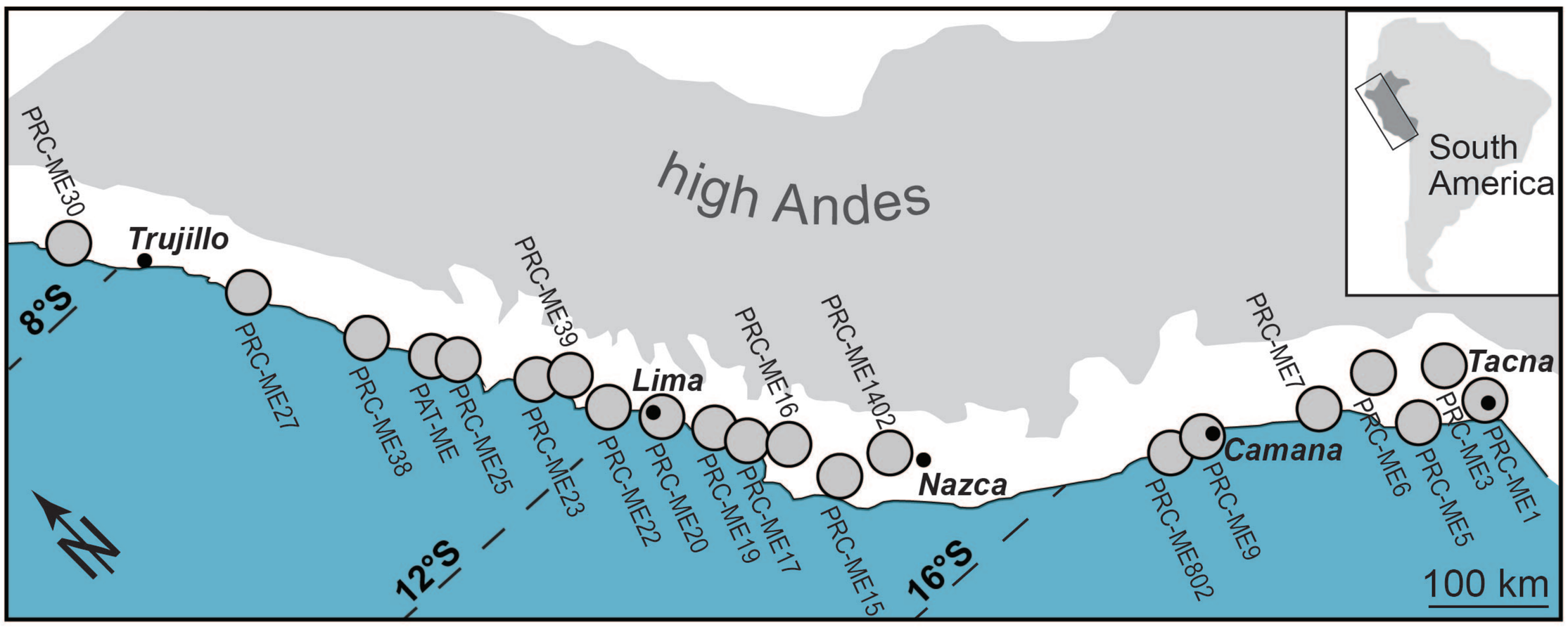
high Andes
South
America
PRC-ME30
Trujillo
PRC-ME27
PRC-ME38
PAT-ME
PRC-ME25
PRC-ME39
PRC-ME23
PRC-ME22
Lima
PRC-ME20
PRC-ME19
PRC-ME16
PRC-ME17
PRC-ME1402
PRC-ME15
Nazca
PRC-ME802
PRC-ME9
Camana
PRC-ME7
PRC-ME6
PRC-ME5
PRC-ME3
Tacna
PRC-ME1
8°S
12°S
16°S
100 km
B

Figure 1

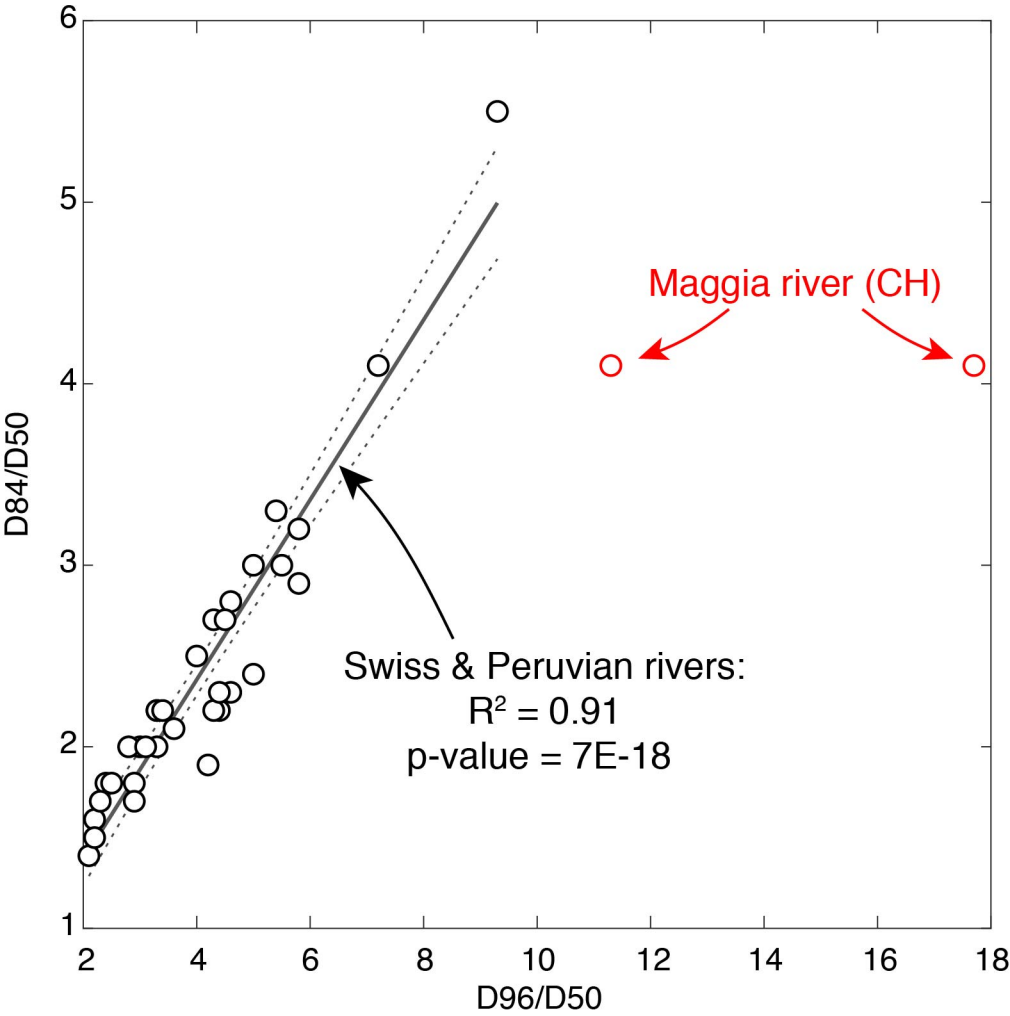
Maggia river (CH)
Swiss & Peruvian rivers:
R² = 0.91
p-value = 7E-18
D84/D50
D96/D50
1
2
3
4
5
6
2
4
6
8
10
12
14
16
18

Figure 2

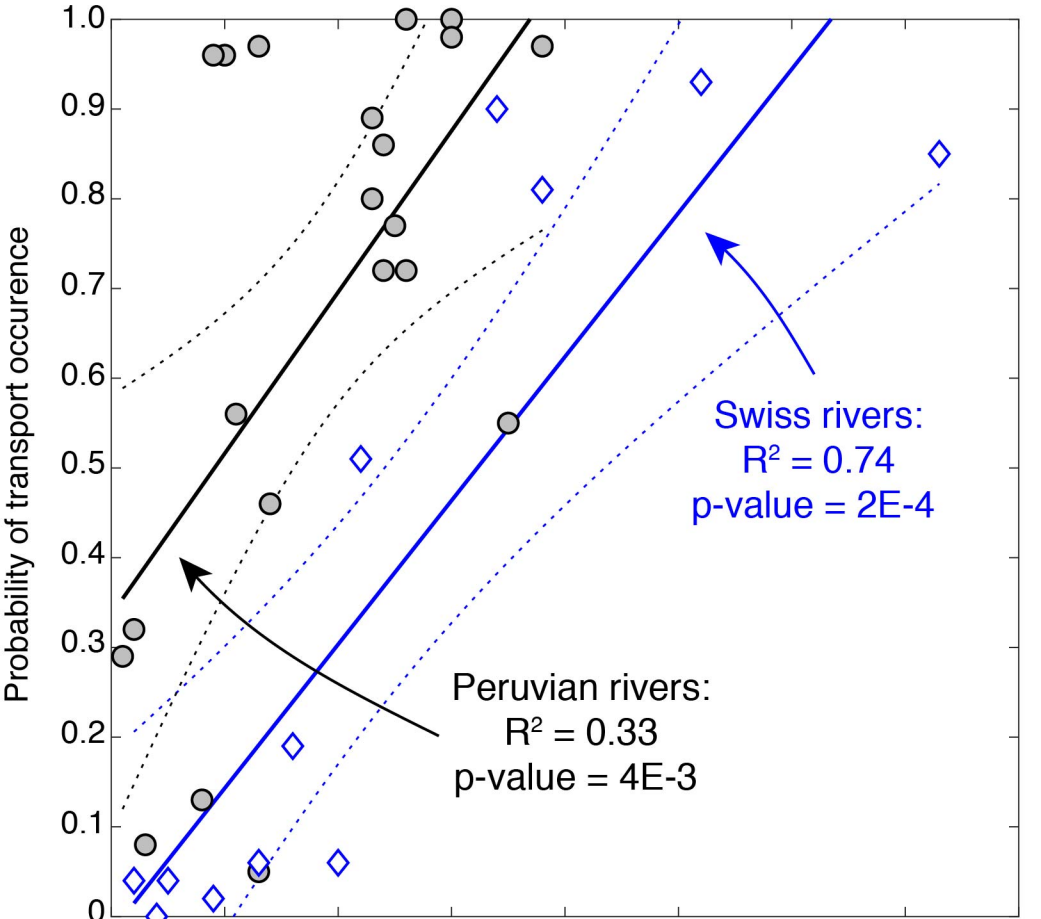
Probability of transport occurence
1.0
0.9
0.8
0.7
0.6
0.5
0.4
0.3
0.2
0.1
0
2
3
4
5
6
7
8
9
10
D96/D50
Swiss rivers:
R² = 0.74
p-value = 2E-4
Peruvian rivers:
R² = 0.33
p-value = 4E-3

Figure 3

TABLE 1. GRAIN SIZE, CHANNEL METRICS, SHEAR STRESSES AND RELATIVE TRANSPORT TIME

Site coordinates Latitude (DD WGS84)	Site coordinates Longitude (DD WGS84)	Channel width along reach (m)	Reach gradient (m/m)	Qmed: Mean annual water discharge (m3/s)	Standard deviation of Qmed (m3/s)	Unit discharge (Q/W; m2/s)	D50 (m)	D84 (m)	D96 (m)	D96/D50	D84/D50	Critical Sheer (median) (Pa)	Critical Sheer (16th%) (Pa)	Critical Sheer (84th%) (Pa)	Sheer stress in response to Qmed (Pa)	Sheer stress in response to Qmed (16th%) (Pa)	Sheer stress in response to Qmed (84th%) (Pa)	Relative transport time for Qmed and the D84 as threshold
46.96	7.75	30	0.007	11.9	2.5	0.4	0.009	0.029	0.052	5.8	3.2	21	15	29	30	23	39	81%
46.98	9.61	32	0.018	24.1	5.1	0.8	0.025	0.083	0.135	5.4	3.3	60	42	82	102	79	130	90%
47.07	8.28	27	0.011	15.5	2.8	0.6	0.009	0.050	0.084	9.3	5.5	36	26	50	55	42	69	85%
46.88	8.62	48	0.007	42.9	4.7	0.9	0.009	0.037	0.064	7.2	4.1	27	19	37	48	38	60	93%
46.17	8.77	84	0.005	22.7	10.8	0.3	0.011	0.046	0.127	11.3	4.1	33	23	46	19	12	26	11%
46.17	8.77	22	0.005	22.7	10.8	1.0	0.008	0.033	0.140	17.7	4.1	24	17	33	39	26	53	83%
47.01	9.30	92	0.002	167.5	24.5	1.8	0.070	0.128	0.169	2.4	1.8	92	65	127	26	20	32	0%
46.36	7.05	24	0.004	21.0	3.9	0.9	0.049	0.080	0.108	2.2	1.6	58	41	80	27	21	35	4%
46.38	7.53	32	0.007	19.0	1.7	0.6	0.061	0.111	0.153	2.5	1.8	80	56	110	39	31	49	4%
47.30	9.12	52	0.002	37.9	6.8	0.7	0.024	0.045	0.069	2.9	1.8	32	23	45	13	10	17	2%
46.39	7.27	15	0.014	12.0	1.8	0.8	0.062	0.119	0.263	4.2	1.9	86	61	118	87	68	109	51%
47.24	9.19	26	0.005	10.2	1.6	0.4	0.028	0.064	0.094	3.3	2.2	46	33	64	24	19	30	6%
46.39	7.40	26	0.009	20.0	2.3	0.8	0.054	0.116	0.193	3.6	2.1	84	59	115	58	46	72	19%
46.89	7.35	24	0.005	8.7	1.7	0.4	0.024	0.060	0.096	4.0	2.5	43	31	60	22	17	28	6%
-18.12	-70.33	6	0.015	3.4	0.8	0.6	0.023	0.062	0.100	4.3	2.7	45	32	62	76	58	97	89%
-17.82	-70.51	6	0.013	4.0	5.0	0.7	0.025	0.055	0.110	4.4	2.2	40	28	55	83	46	126	86%
-17.29	-70.99	7	0.018	3.4	1.0	0.5	0.026	0.051	0.078	3.0	2.0	37	26	51	82	61	107	96%
-17.03	-71.69	26	0.051	38.1	37.8	1.5	0.015	0.036	0.075	5.0	2.4	26	18	36	432	244	643	100%
-16.34	-72.13	15	0.019	30.1	21.7	2.0	0.020	0.060	0.100	5.0	3.0	43	31	60	193	116	278	98%
-16.51	-72.64	100	0.005	68.4	52.7	0.7	0.052	0.087	0.120	2.3	1.7	63	44	86	31	18	45	8%
-16.42	-73.12	70	0.004	91.1	82.2	1.3	0.048	0.068	0.100	2.1	1.4	49	35	68	37	21	54	29%
-15.85	-74.26	3	0.014	20.4	29.9	6.8	0.013	0.030	0.060	4.6	2.3	22	15	30	336	182	510	100%
-15.63	-74.64	23	0.003	12.1	16.7	0.5	0.029	0.064	0.096	3.3	2.2	46	33	64	19	10	29	5%
-13.73	-75.89	20	0.013	13.6	17.8	0.7	0.030	0.066	0.130	4.3	2.2	48	34	66	85	47	129	80%
-13.47	-76.14	5	0.010	10.1	14.8	2.0	0.013	0.038	0.076	5.8	2.9	28	19	38	126	68	191	97%
-13.12	-76.39	60	0.010	26.4	25.9	0.4	0.020	0.046	0.088	4.4	2.3	33	23	46	49	28	72	72%
-12.67	-76.65	22	0.008	8.2	9.8	0.4	0.016	0.048	0.088	5.5	3.0	35	25	48	38	21	57	55%
-12.25	-76.89	5	0.022	3.7	4.3	0.7	0.030	0.050	0.088	2.9	1.7	36	26	50	141	78	212	96%
-11.79	-76.99	40	0.018	4.9	5.1	0.1	0.053	0.105	0.150	2.8	2.0	76	54	104	42	24	63	13%
-11.61	-77.24	20	0.010	8.9	7.8	0.4	0.055	0.083	0.120	2.2	1.5	60	42	82	48	27	70	32%
-11.07	-77.59	5	0.012	3.8	4.6	0.8	0.028	0.077	0.130	4.6	2.8	56	39	77	82	45	124	72%
-10.72	-77.77	30	0.014	30.9	24.3	1.0	0.018	0.036	0.060	3.3	2.0	26	18	36	102	60	148	97%
-10.07	-78.16	15	0.004	9.8	12.7	0.7	0.017	0.034	0.052	3.1	2.0	25	17	34	28	15	42	56%
-8.97	-78.62	40	0.005	96.1	67.7	2.4	0.020	0.054	0.090	4.5	2.7	39	27	54	61	37	87	77%
-7.32	-79.48	40	0.007	25.4	27.7	0.6	0.029	0.063	0.100	3.4	2.2	45	32	63	44	24	65	46%

in=Peruvian Rivers

om the Swiss Rivers is taken from the Swiss Federal Office for the Environment (FOEN: www. hydrodaten.admin.ch). Reported values represent discharges monitored over the period 1990-2011; Except for the Rhein (1977-1990).

ainage basin size data from the Peruvian Rivers is taken from Reber et al. (2017) and Litty et al. (2017)

m the Peruvian streams is taken from Litty et al. (2017)

annel width and gradient data from the Emme, Landquart, Reuss, Maggia and Sense Rivers is taken from Litty and Schlunegger (2017)